Measurement of the Higgs boson mass by ATLAS and CMS[†]

ATLAS part

Ruggero Turra

Univ. Studi di Milano & INFN
On behalf of the ATLAS Collaboration

Workshop on Higgs Couplings
Torino (Italy)

Oct 1, 2014

ATLAS Collaboration, "Measurement of the Higgs boson mass from the $H \to \gamma\gamma$ and $H \to ZZ^* \to 4\ell$ channels with the ATLAS detector using 25 fb^{-1} of pp collision data", Phys. Rev. D **90** (2014) 052004 arXiv:1406.3827 [hep-ex].

ATLAS Collaboration, "Electron and photon energy calibration with the ATLAS detector using LHC Run 1 data", arXiv:1407.5063 [hep-ex].

ATLAS Collaboration, "Measurement of the muon reconstruction performance of the ATLAS detector using 2011 and 2012 LHC proton-proton collision data", arXiv:1407.3935 [hep-ex].

[†] See Arabella Martelli talk

Introduction

Results are based on full LHC Run1 at $\sqrt{s} = 7$ and 8 TeV.

$H \to \gamma\gamma$:

- small branching ratio ($\sim 10^{-3}$)
- simple signature: two isolated photons with large transverse momentum
- huge background: $\gamma\gamma$, γj, jj, Drell-Yan. $s/b \simeq 3.4\%$ in $\pm\sigma_{eff\,90}$

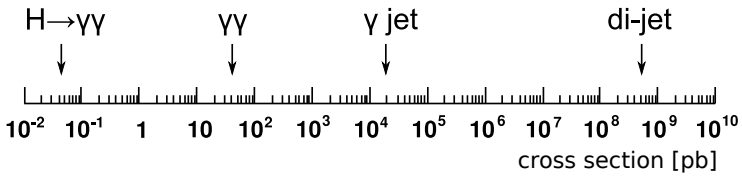

$H \to ZZ \to 4\ell$:

- very small branching ratio ($\sim 10^{-4}$)
- golden channel: very small backgrounds (diboson, Zj, $t\bar{t}$): $s/b \simeq 2$ (in 120-130 GeV)
- measurement dominated by 4μ channel
- possibility to apply Z mass constraint

Mass measurement dominated by energy scale

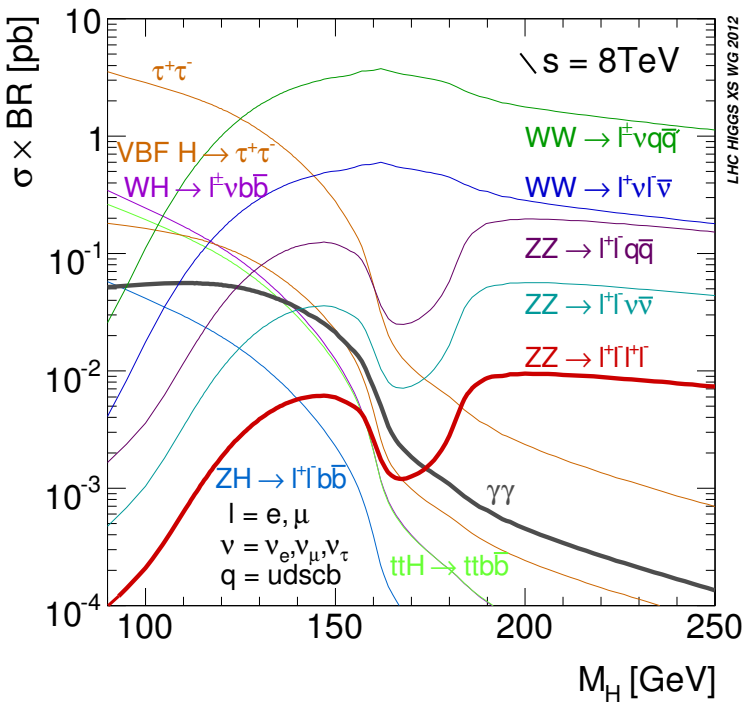

Introduction

Results are based on full LHC Run1 at $\sqrt{s} = 7$ and 8 TeV.

$H \to \gamma\gamma$:

- small branching ratio ($\sim 10^{-3}$)
- simple signature: two isolated photons with large transverse momentum
- huge background: $\gamma\gamma$, γj, jj, Drell-Yan. $s/b \simeq 3.4\%$ in $\pm\sigma_{eff90}$

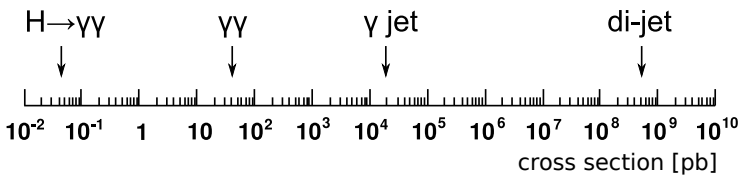

$H \to ZZ \to 4\ell$:

- very small branching ratio ($\sim 10^{-4}$)
- golden channel: very small backgrounds (diboson, Zj, $t\bar{t}$): $s/b \simeq 2$ (in 120-130 GeV)
- measurement dominated by 4μ channel
- possibility to apply Z mass constraint

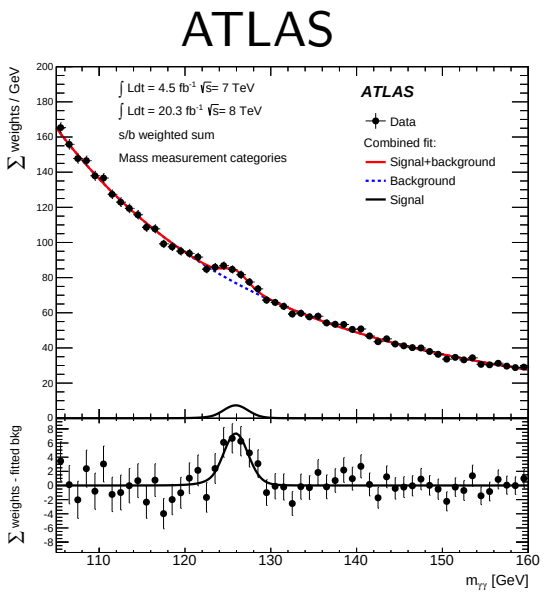

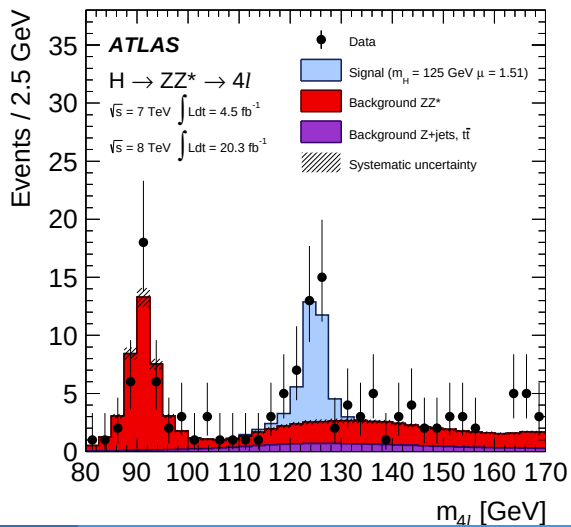

Introduction

Results are based on full LHC Run1 at $\sqrt{s} = 7$ and 8 TeV.

$H \to \gamma\gamma$:

- small branching ratio ($\sim 10^{-3}$)
- simple signature: two isolated photons with large transverse momentum
- huge background: $\gamma\gamma$, γj, jj, Drell-Yan. $s/b \simeq 3.4\%$ in $\pm\sigma_{eff90}$

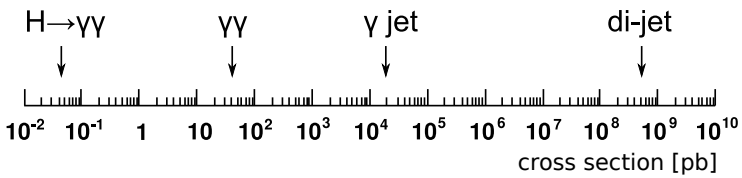

$H \to ZZ \to 4\ell$:

- very small branching ratio ($\sim 10^{-4}$)
- golden channel: very small backgrounds (diboson, Zj, $t\bar{t}$): $s/b \simeq 2$ (in 120-130 GeV)
- measurement dominated by 4μ channel
- possibility to apply Z mass constraint

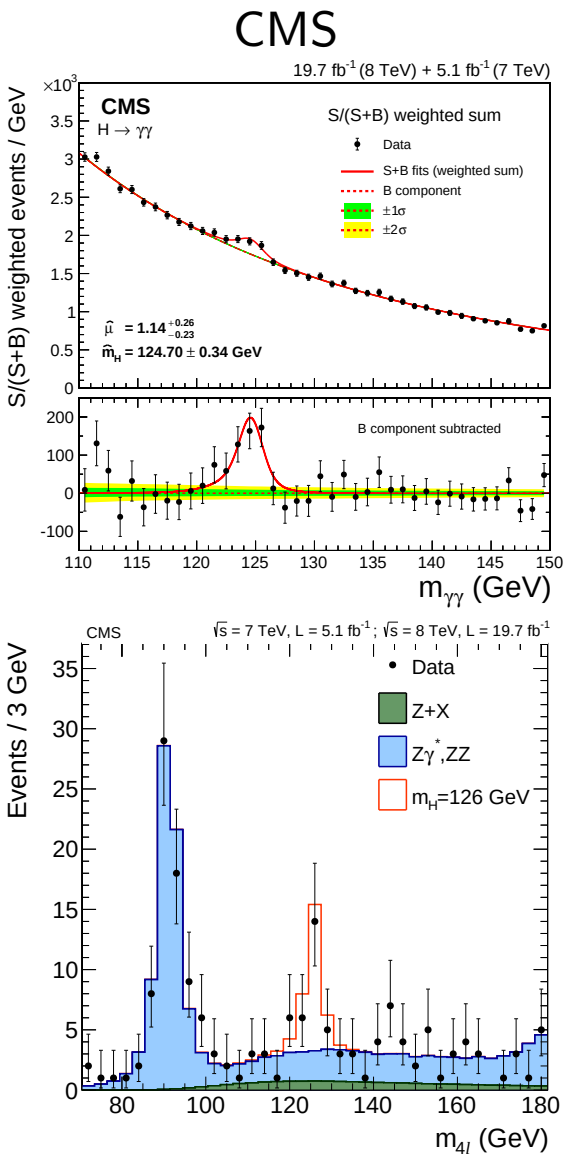

Muon momentum calibration

- p_T is measured by Inner Detector (ID) ($|\eta| < 2.5$) and MS Spectrometer (MS) ($0.1 < |\eta| < 2.7$).
- p_T-scale corrected comparing simulation and data $J/\psi/Z \to \mu\mu$
- combining ID and MS, systematics on p_T-scale 0.04% (barrel) $\div$ 0.2% ($|\eta| > 2$)
  - new inclusion of J/ψ allows for a significant reduction in the $H \to 4\ell$ p_T-region

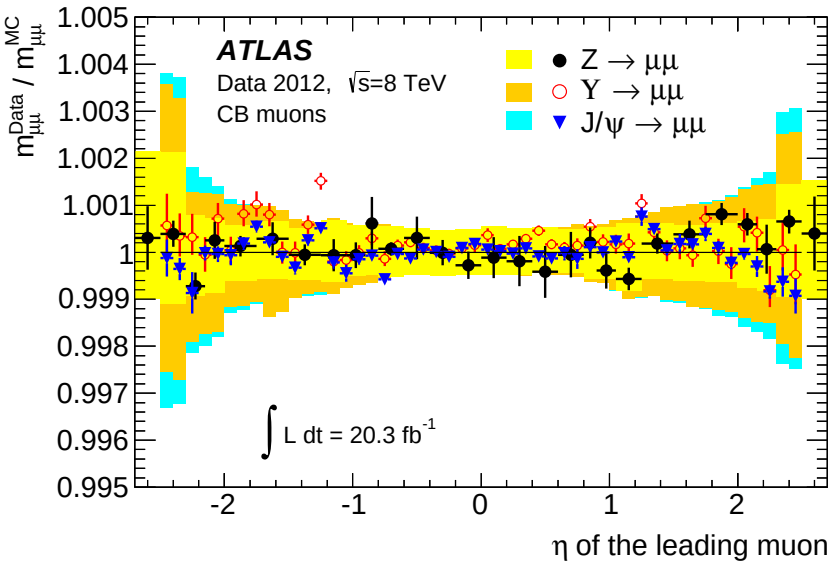

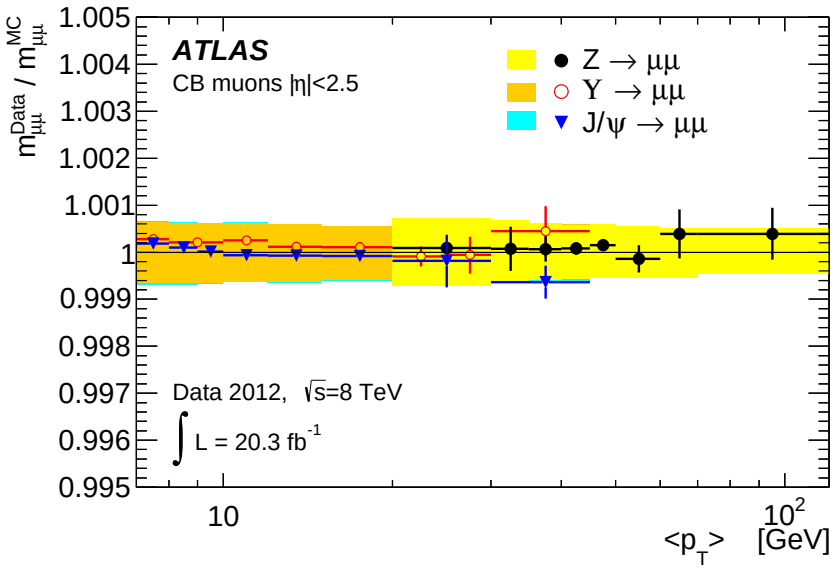

- p_T-dependent smearing correction to match resolution in data

e/γ energy calibration

- Energy collected in rectangular fixed-size cluster of calorimetric cells
  - Larger window for converted photons

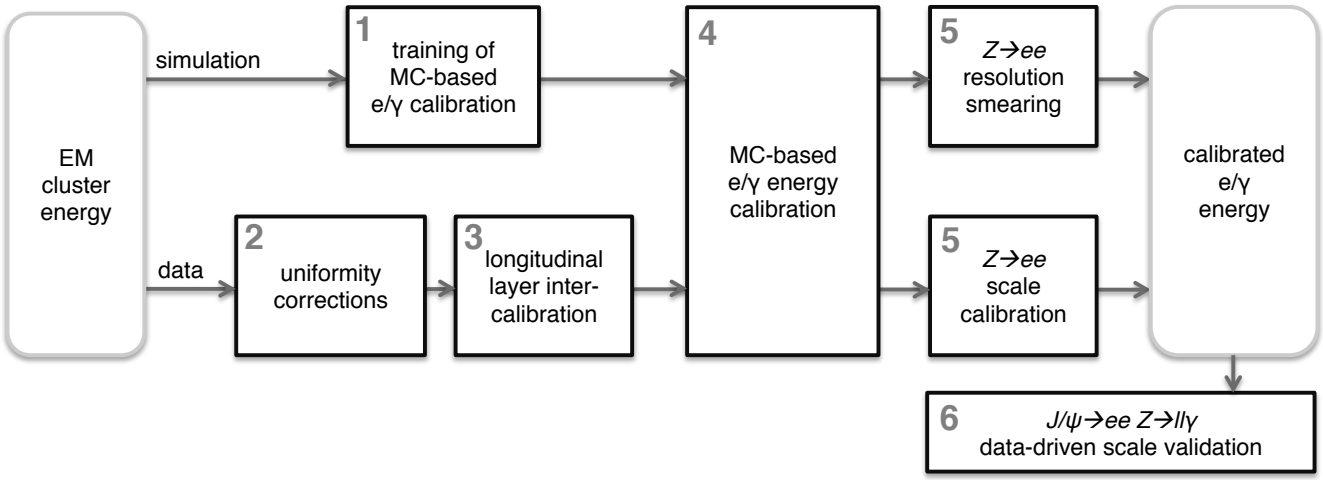

- (2+3) Very detailed data-driven corrections on the cluster energy (HV, deformation effects, gain, presampler, E_1/E_2 correction) using $Z \to ee$, $Z \to \mu\mu$, photons
- (4) New MVA MC-based calibration using as input: position, shower depth, presampler, radius of conversion
  - different calibration for electron / converted / unconverted photons
- (5) scale factors and smearing comparing $Z \to ee$ data/MC: as a function of $|\eta|$
  - applied both on electrons and photons
- *E-p* combination used for low p_T electrons: $H \to 4e/2\mu 2e/2e2\mu$

- Residual scale factors extracted also as function of p_T to check linearity
  - no additional systematics needed
- Residual scale factors extracted from $Z \to ll\gamma$ (limited by statistics)
  - no additional systematics needed

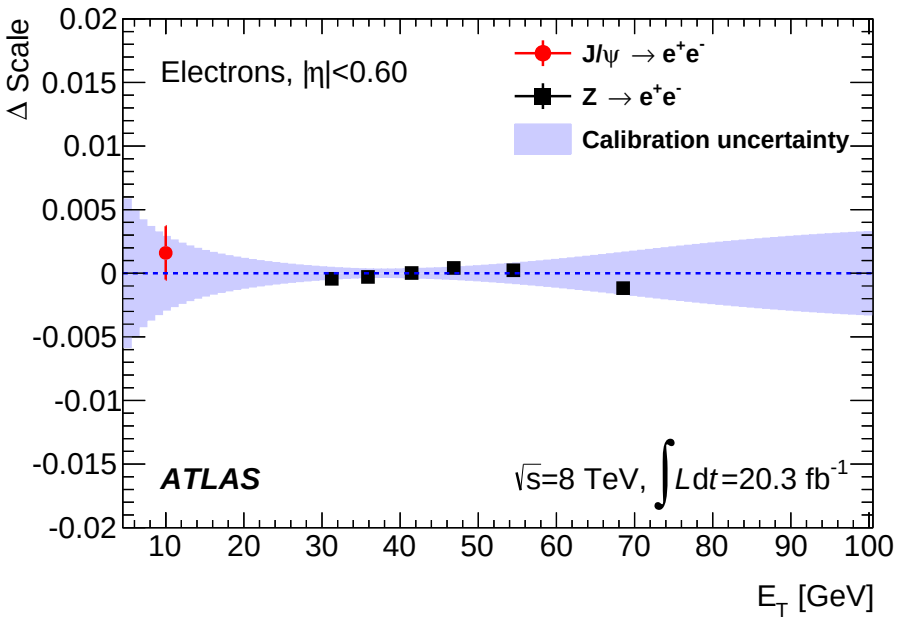

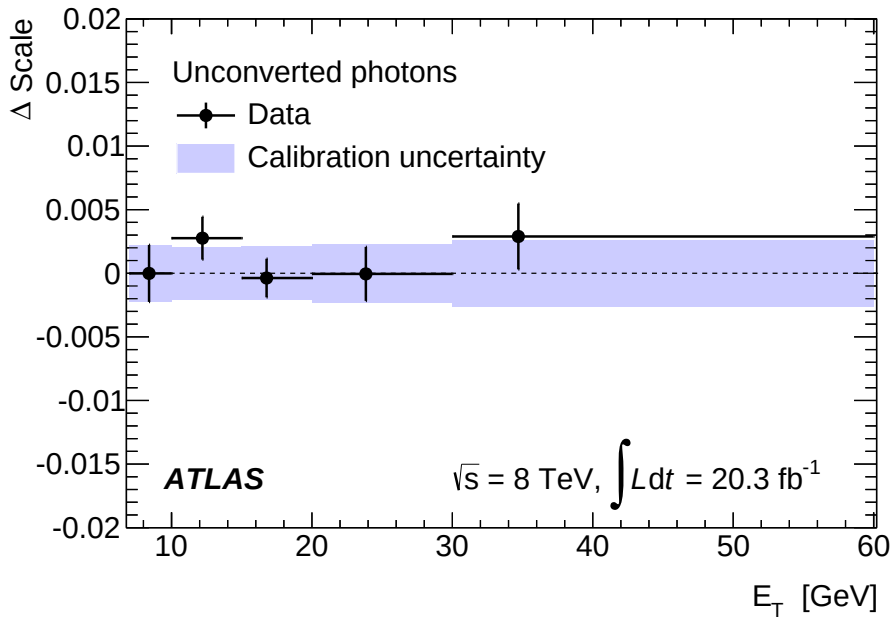

- Two isolated high-energy photons with $p_{T_{1,2}}/m_{\gamma\gamma} > 0.35, 0.25$
- Good diphoton purity after cuts: $\simeq 75\%$
- Vertex position using calorimetric pointing: z-vertex resolution 15 mm
- NN to select primary vertex: 93% efficiency within ± 15 mm (plot for 0.3 mm)
- 10 categories detector-based using conversion status / η / p_{Tt}, based on resolution and s/b.

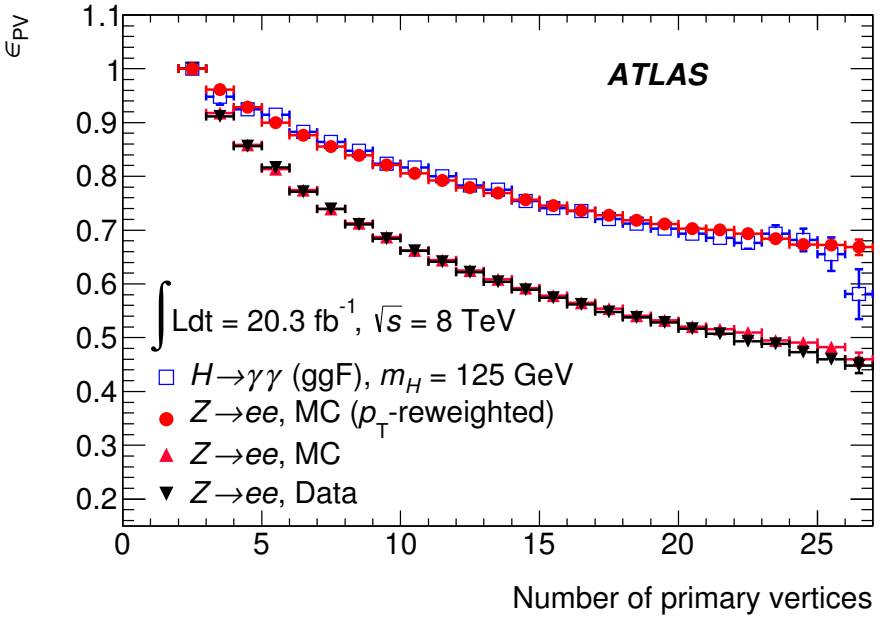

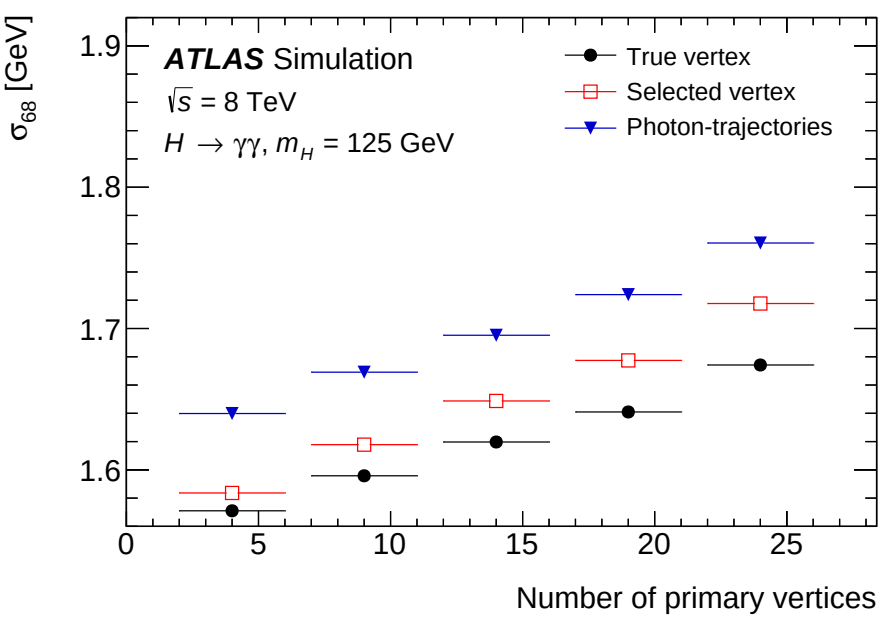

Signal:

- from simulation: Gaussian + Crystal Ball
- resolution $\simeq$ 1.7 GeV

Background:

- fitted on data using a predefined function (e.g. exponential, . . .)
- functional form selected minizing the spurious signal
- spurious signal evaluated with s+b fit on a very high stat background MC

Systematic from the background:

- Systematic on m_H estimated in a similar way using a S+B fit on the same background MC + injected Asimov signal.
- Taking the maximum difference between injected and fitted m_H in [119, 135] GeV used as systematic (pessimistic procedure): $0.05\% \div 0.2\%$

m_H estimated with a maximum profiled likelihood fit, with systematics implemented as nuisance parameters

$$m_H = 125.98 \pm 0.42(\text{stat}) \pm 0.28(\text{sys})\ \text{GeV}$$
$$\text{previous} \quad m_H = 126.8 \pm 0.2(\text{stat}) \pm 0.7(\text{sys})\ \text{GeV}$$

- Systematics dominated by energy scale, reduced by a factor 2.5
  - most important: Lar cell non-linearity, material, lateral shower shape photon/electron differences
  - mass resolution uncertainty: $9 - 16\%$, negligible impact

	Unconverted					Converted				
	Central		Rest		Transition	Central		Rest		Transition
Class	low p_{Tt}	high p_{Tt}	low p_{Tt}	high p_{Tt}		low p_{Tt}	high p_{Tt}	low p_{Tt}	high p_{Tt}	
$Z \to e^+e^-$ calibration	0.02	0.03	0.04	0.04	0.11	0.02	0.02	0.05	0.05	0.11
LAr cell nonlinearity	0.12	0.19	0.09	0.16	0.39	0.09	0.19	0.06	0.14	0.29
Layer calibration	0.13	0.16	0.11	0.13	0.13	0.07	0.10	0.05	0.07	0.07
ID material	0.06	0.06	0.08	0.08	0.10	0.05	0.05	0.06	0.06	0.06
Other material	0.07	0.08	0.14	0.15	0.35	0.04	0.04	0.07	0.08	0.20
Conversion reconstruction	0.02	0.02	0.03	0.03	0.05	0.03	0.02	0.05	0.04	0.06
Lateral shower shape	0.04	0.04	0.07	0.07	0.06	0.09	0.09	0.18	0.19	0.16
Background modeling	0.10	0.06	0.05	0.11	0.16	0.13	0.06	0.14	0.18	0.20
Vertex measurement	0.03									
Total	0.23	0.28	0.24	0.30	0.59	0.21	0.25	0.27	0.33	0.47

- Statistical error compatible with expectations: 0.35 GeV for $\mu = 1.3$ (0.45 GeV for $\mu = 1$). Previous: $\mu = 1.6$, expected stat. erro 0.33 GeV.
- Fraction of pseudo-experiments with a statistical error larger than the one observed in data is 16%
- Compatibility between different categories (using conversion status / number of primary vertexes / detector region): deviation $< 1.5\sigma$
- Expected shift on the mass due to the new calibration

$H \to 4\ell$

- electron (muon) $p_T > (6)7$ GeV
- four categories: $4e$, $2\mu 2e$, $2e2\mu$, 4μ
- New neural network for electron identification
- E/p combination for electron $p_T < 30$ GeV: improvement resolution 4% $(4e, 2\mu 2e)$
- New multivariate discriminant for ZZ^* background
- collinear (and non-collinear) FSR photon recovery: correction 4 (1) %
- Z mass constraint on the leading pair: 15% resolution improvement

Background estimation:

- ZZ from simulation
- other data-driven

Signal:

- simulation smoothed with kernel density estimation
- resolution (gaussian core): 1.6 GeV (4μ), 1.7 GeV ($2\mu 2e$), 2.2 GeV ($4e$)

Model:

- 2D model of $m_{4\ell}$ and BDT_{ZZ}
- BDT_{ZZ} trained to discriminate between ZZ and signal (based on matrix element-based kinematic discriminant)
- cross check with:
  - model using only $m_{4\ell}$
  - analysis using per-event-error (and no Z mass constraint)

$$m_H = 124.51 \pm 0.52(\text{stat}) \pm 0.06(\text{sys})\ \text{GeV}$$

$$\text{previous} \quad m_H = 124.3^{+0.6}_{-0.5}(\text{stat})^{+0.5}_{-0.3}\ \text{GeV}$$

- 8% improvement with respect to simple 1D fit (only $m_{4\ell}$ mass)
- good compatibility between categories ($< 2\sigma$)
- 26.5 event expected, 37 observed
- similar systematics from muon and electron scale: $\pm 0.03\%$ both

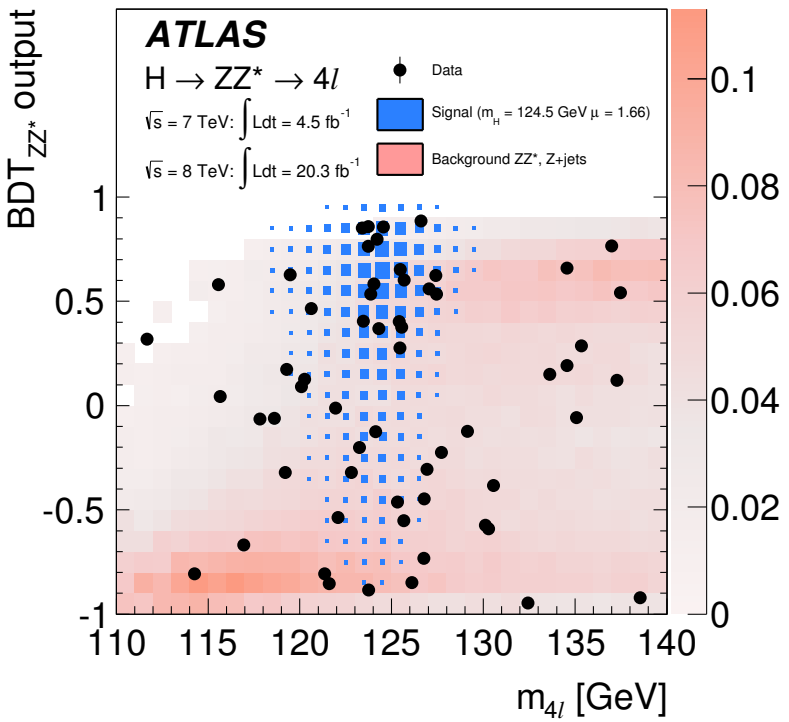

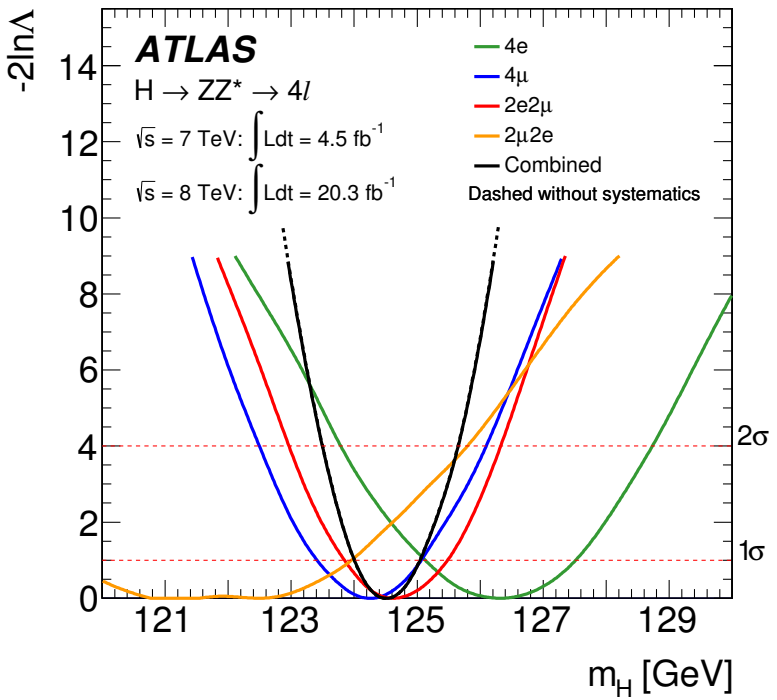

ATLAS Combination

$$m_H = 125.36 \pm 0.37(\text{stat}) \pm 0.18(\text{sys})\ \text{GeV}$$

$$\text{previous} \quad m_H = 125.49 \pm 0.24(\text{stat})^{+0.50}_{-0.58}(\text{sys})\ \text{GeV}$$

- Systematics reduced by a factor 3
- $\mu_{4\ell}$ and $\mu_{\gamma\gamma}$ as independent nuisance parameters
- e/γ energy scale fully correlated
- Compatibility between channels 2.0σ (p-value $= 4.8\%$) with free $\mu_{4\ell}$ and $\mu_{\gamma\gamma}$
- Compatibility 1.6σ forcing $\mu_{4\ell} = \mu_{\gamma\gamma} = 1$

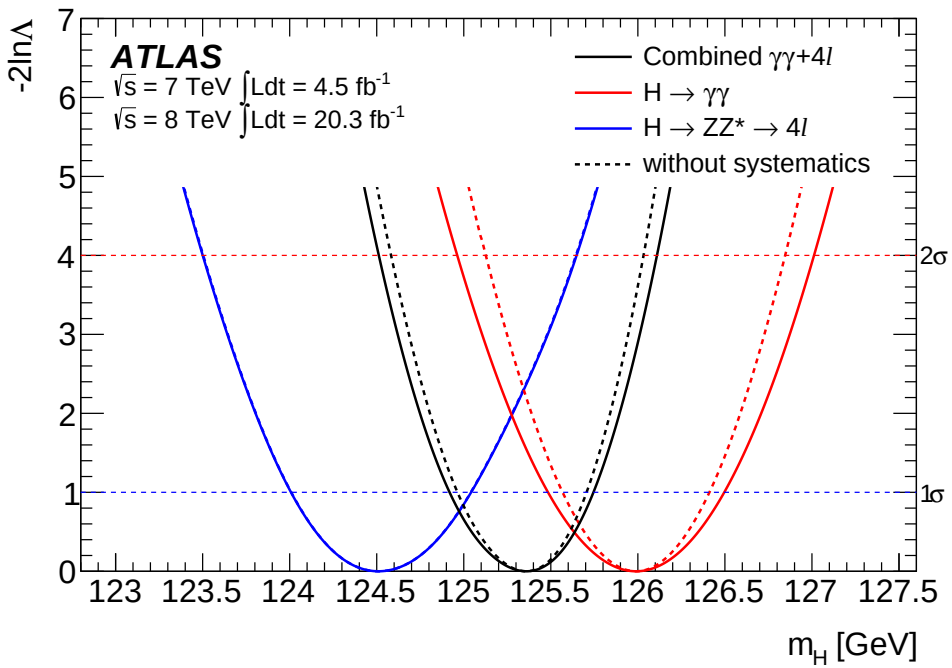

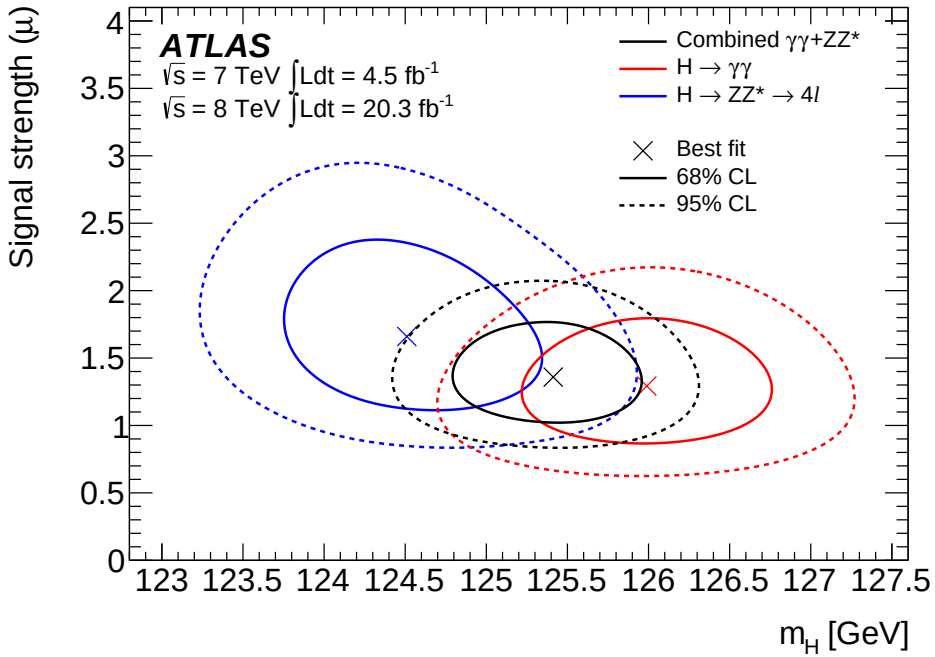

Section 1

Backup

- Energy collected in rectangular cluster of calorimetric cells
  - Larger window for converted photons
- Cell energy calibration from periodic electronic calibration run.
  - Stability of calorimeter response versus time: $< 0.05\%$
- residual correction for non-nominal HV (few sectors of the calorimeter) using azimuthal profiles of $Z \to ee$
- similar correction for few sectors in the presampler
- gravity-induced widening of the inter-module gaps in the barrel

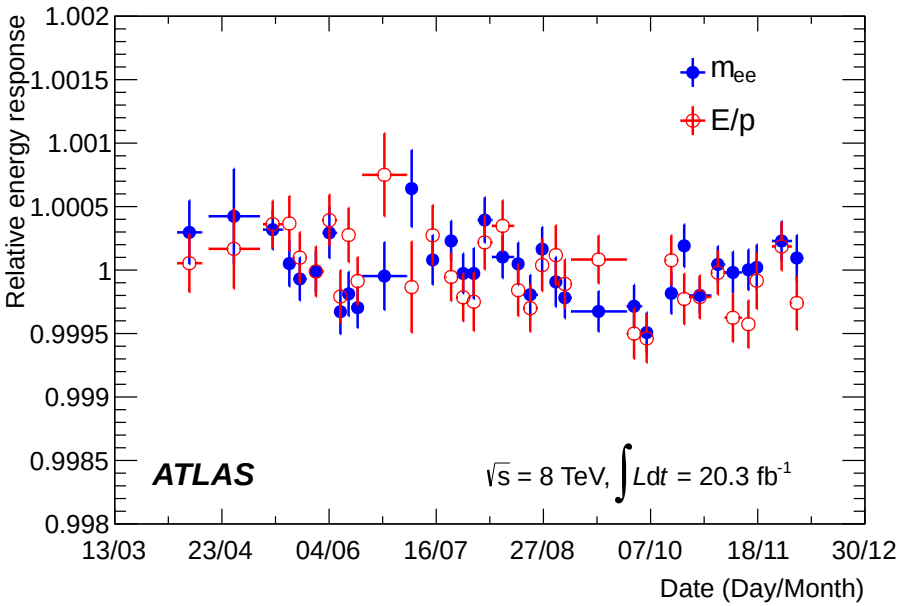

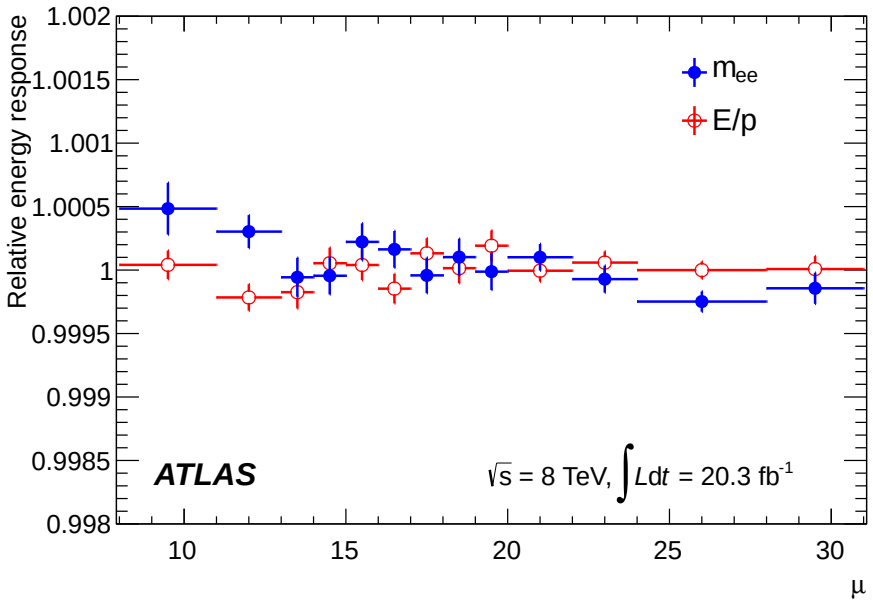

- Energy collected in rectangular cluster of calorimetric cells
  - Larger window for converted photons
- Cell energy calibration from periodic electronic calibration run.
  - Stability of calorimeter response versus time: $< 0.05\%$
- residual correction for non-nominal HV (few sectors of the calorimeter) using azimuthal profiles of $Z \rightarrow ee$
- similar correction for few sectors in the presampler
- gravity-induced widening of the inter-module gaps in the barrel

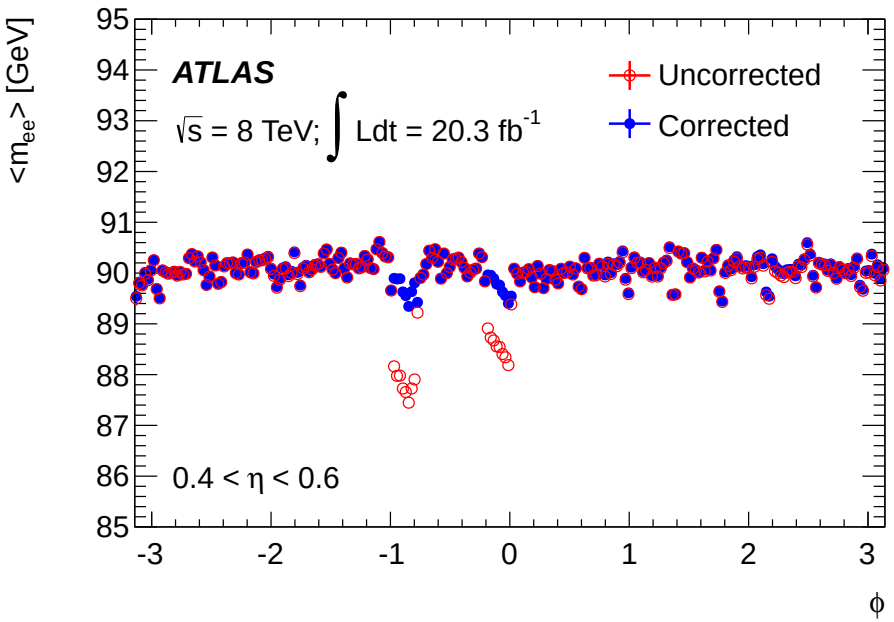

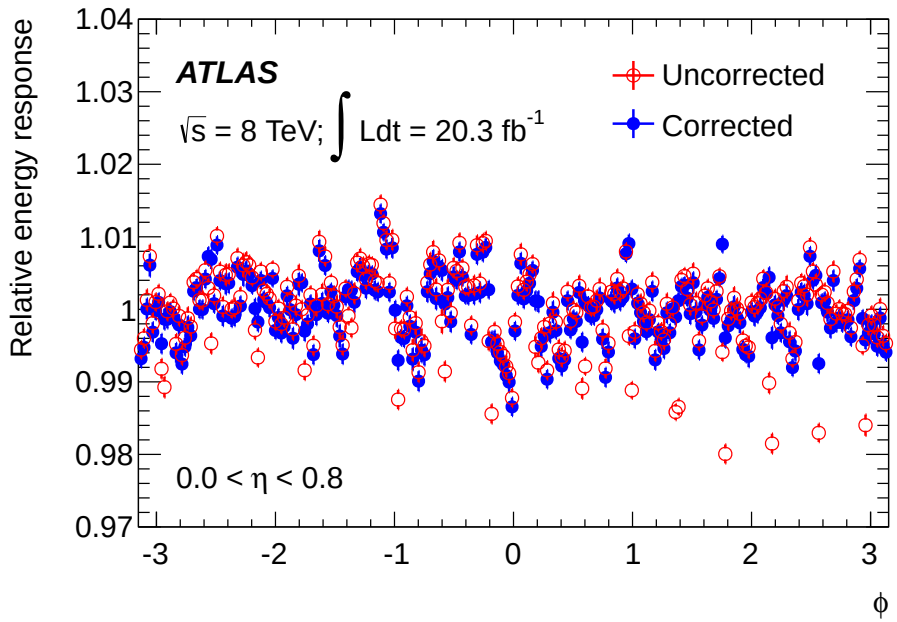

- One of the most important systematics for $H \to \gamma\gamma$
- Most electrons from $Z \to ee$ (used to derive the calibration) are in high-gain
- 1/3 of the photons from $H \to \gamma\gamma$ have at least one cell in medium-gain
- comparing electrons with all cells in HG with electrons with electron with at least 1 MG cell
- non-negligible difference, correction applied

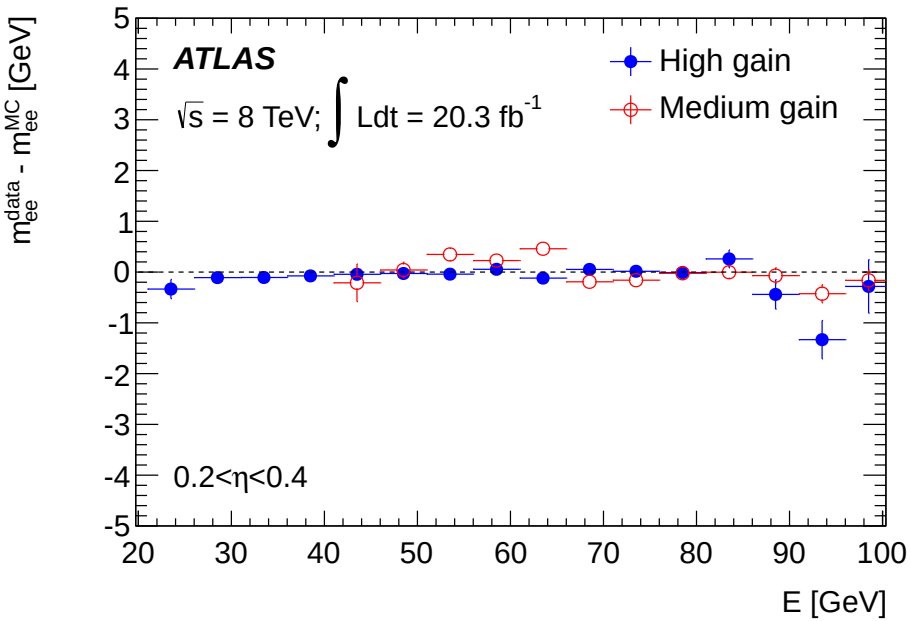

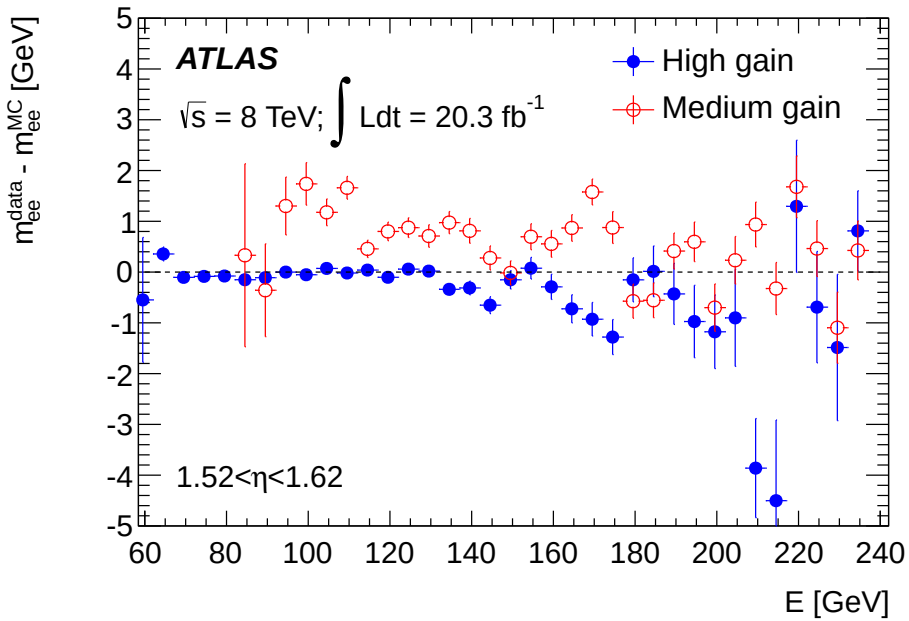

- New E_1/E_2 scale
  - Using $Z \to \mu\mu$ energy loss in calorimeter, comparing data/MC
  - muons not sensitive to material $\to$ intrinsic layer scale
  - correction $\simeq 2\%$
  - systematics $1 \div 2\%$
- New presampler scale
  - Using $Z \to ee$, comparing the presampler energy in data and simulation as a function of the longitudinal shower
  - systematics $< 5\%$
- New MVA MC-based calibration (10% improvement on $m_{\gamma\gamma}$ resolution).
  - different for electron / converted / unconverted photons
  - energy in the calorimeter, presampler fraction, longitudinal shower-depth, $|\eta|$ of the cluster and local position of the shower within the second-layer cell corresponding to the cluster centroid. For converted photons the track transverse momenta and the conversion radius.
- Energy scale from $Z \to ee$

Systematics low p_T using J/ψ

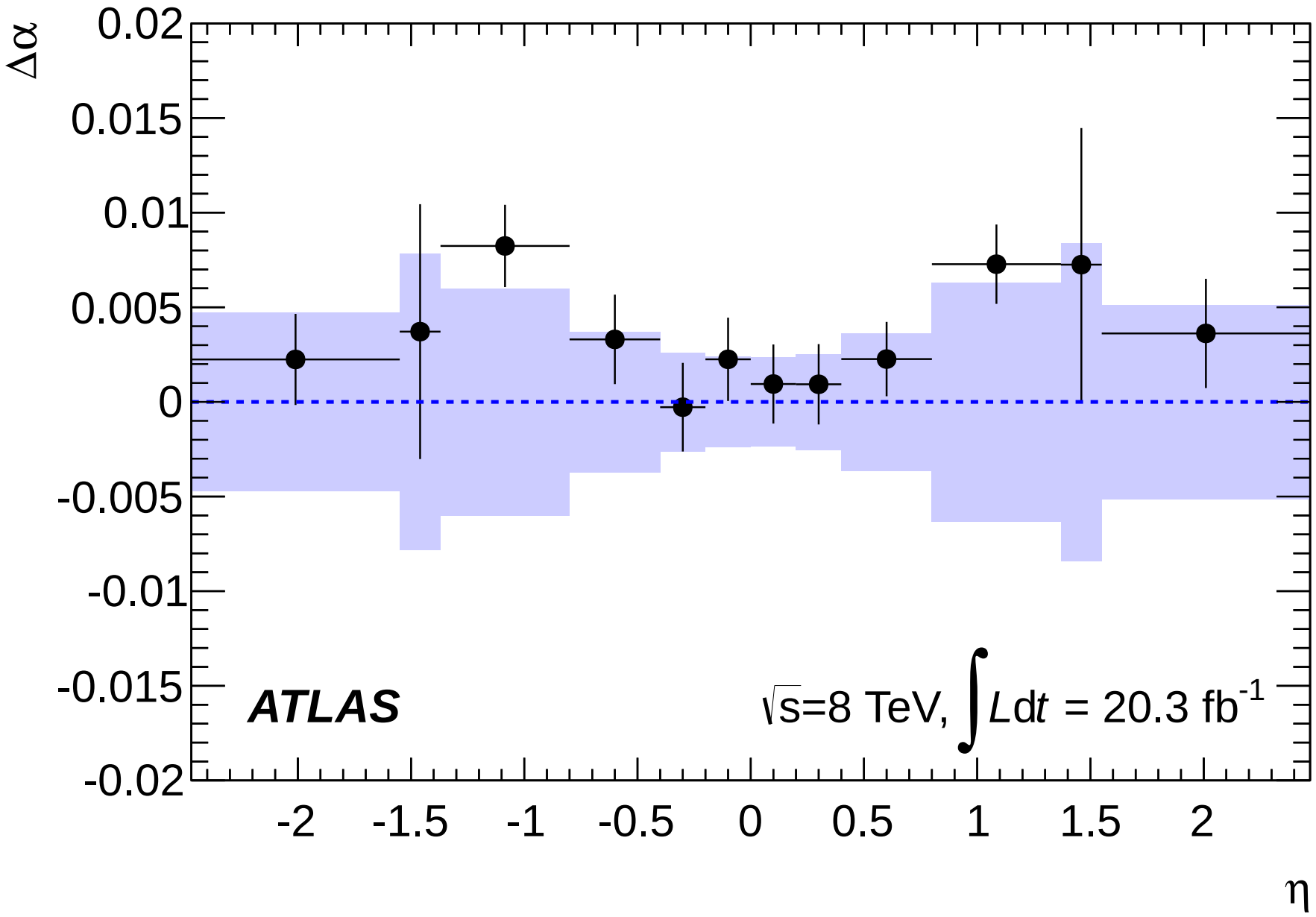

Material

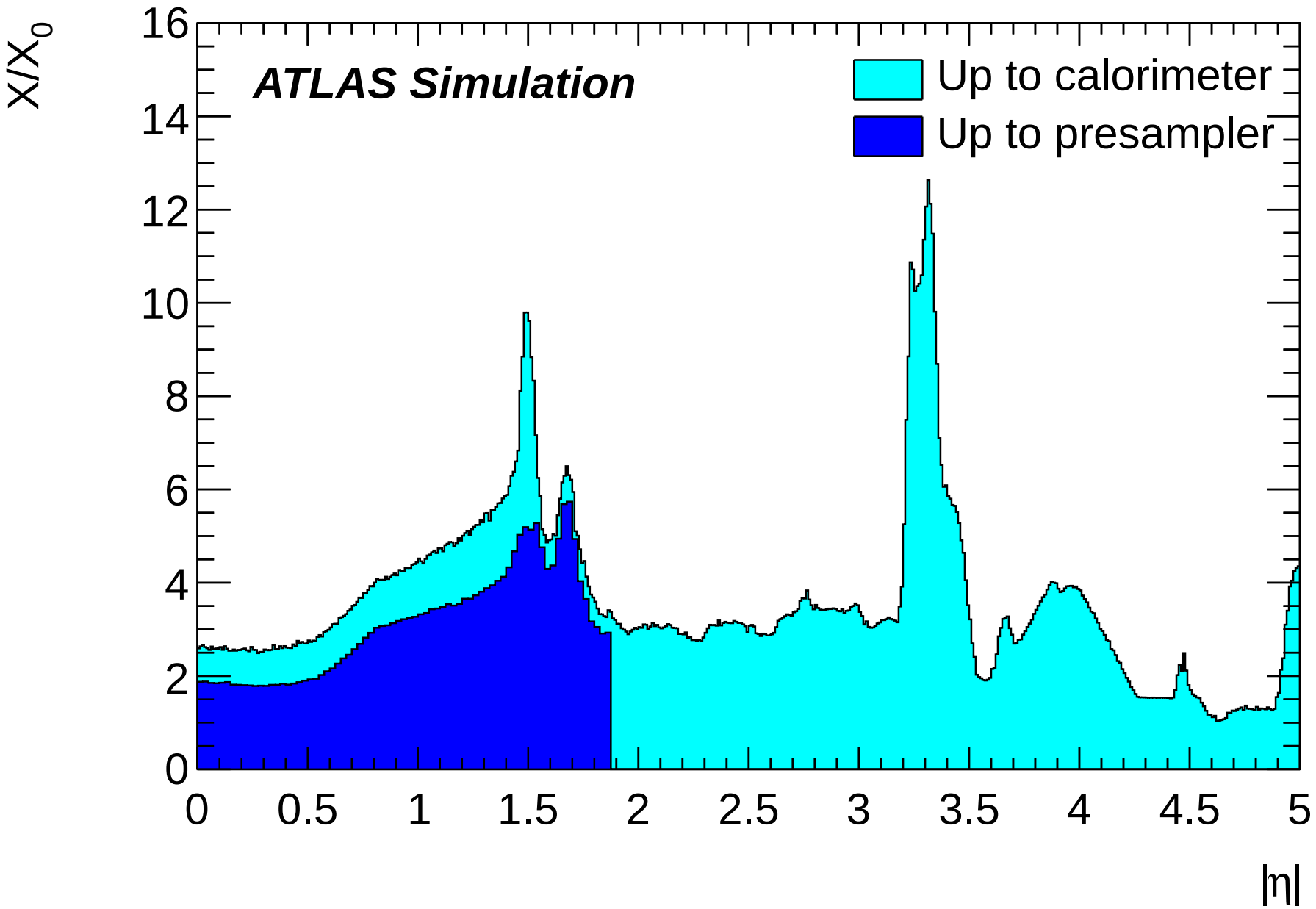
X/X0
ATLAS Simulation
Up to calorimeter
Up to presampler
16
14
12
10
8
6
4
2
0
0
0.5
1
1.5
2
2.5
3
3.5
4
4.5
5
|η|

Material improvement

- Material investigated with E_1/E_2 using electron / unconverted photons in different regions
- New geometry with better matching between data/simulation
- Decoupling of the material effect in different regions

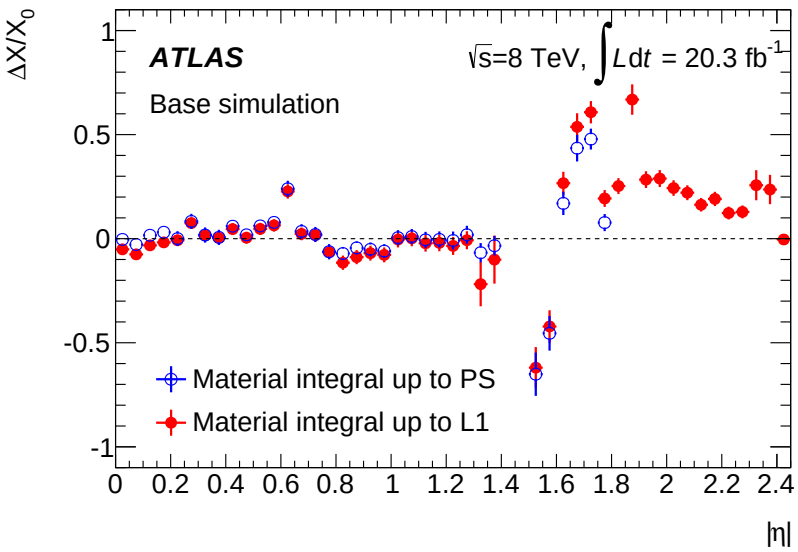

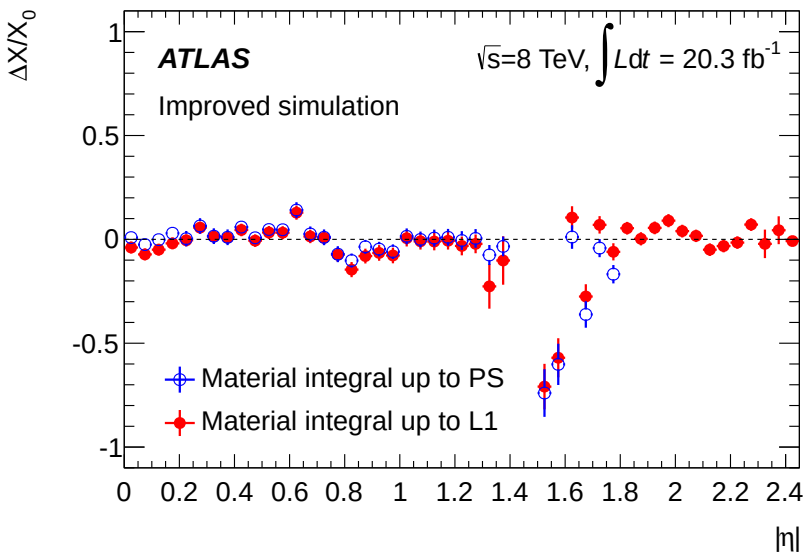

Systematics $H \to \gamma\gamma$

	Unconverted					Converted				
	Central		Rest		Transition	Central		Rest		Transition
Class	low p_{Tt}	high p_{Tt}	low p_{Tt}	high p_{Tt}		low p_{Tt}	high p_{Tt}	low p_{Tt}	high p_{Tt}	
$Z \to e^+e^-$ calibration	0.02	0.03	0.04	0.04	0.11	0.02	0.02	0.05	0.05	0.11
LAr cell nonlinearity	0.12	0.19	0.09	0.16	0.39	0.09	0.19	0.06	0.14	0.29
Layer calibration	0.13	0.16	0.11	0.13	0.13	0.07	0.10	0.05	0.07	0.07
ID material	0.06	0.06	0.08	0.08	0.10	0.05	0.05	0.06	0.06	0.06
Other material	0.07	0.08	0.14	0.15	0.35	0.04	0.04	0.07	0.08	0.20
Conversion reconstruction	0.02	0.02	0.03	0.03	0.05	0.03	0.02	0.05	0.04	0.06
Lateral shower shape	0.04	0.04	0.07	0.07	0.06	0.09	0.09	0.18	0.19	0.16
Background modeling	0.10	0.06	0.05	0.11	0.16	0.13	0.06	0.14	0.18	0.20
Vertex measurement	0.03									
Total	0.23	0.28	0.24	0.30	0.59	0.21	0.25	0.27	0.33	0.47

Systematics on combination

Systematic	Uncertainty on m_H [MeV]
LAr syst on material before presampler (barrel)	70
LAr syst on material after presampler (barrel)	20
LAr cell nonlinearity (layer 2)	60
LAr cell nonlinearity (layer 1)	30
LAr layer calibration (barrel)	50
Lateral shower shape (conv)	50
Lateral shower shape (unconv)	40
Presampler energy scale (barrel)	20
ID material model ($\|\eta\| < 1.1$)	50
$H \to \gamma\gamma$ background model (unconv rest low p_{Tt})	40
$Z \to ee$ calibration	50
Primary vertex effect on mass scale	20
Muon momentum scale	10
Remaining systematic uncertainties	70
Total	180

Pulls

1σ effect and pull

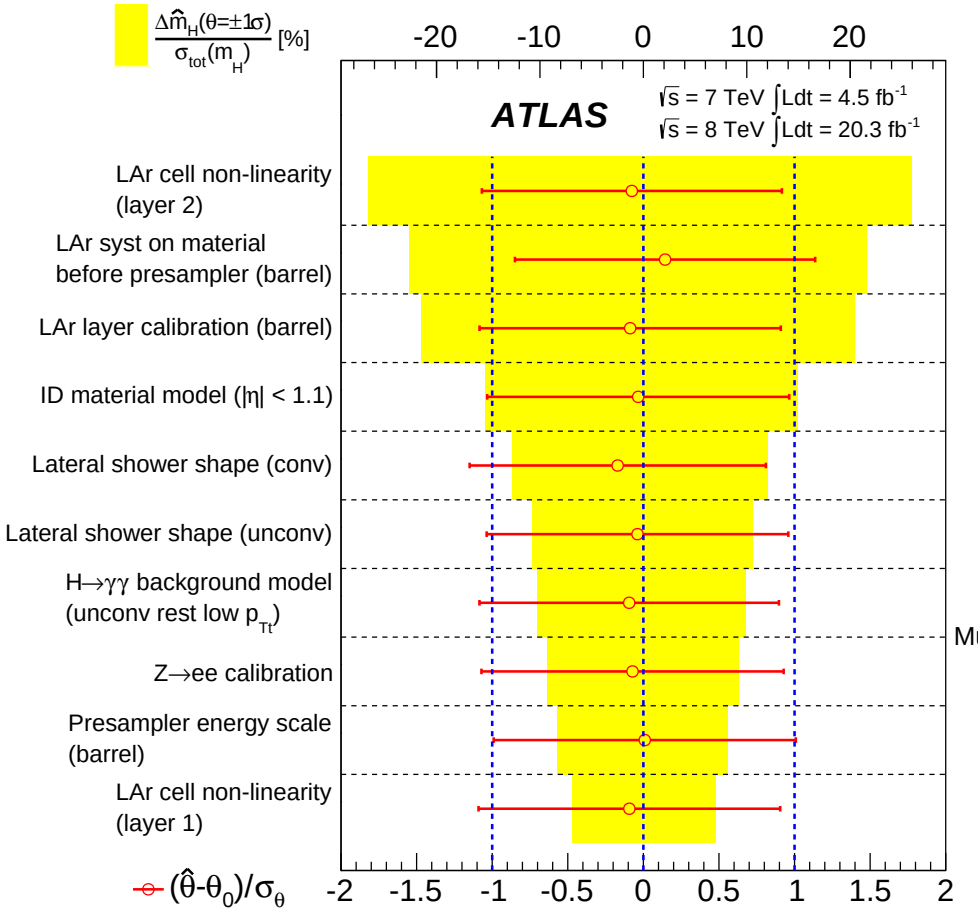

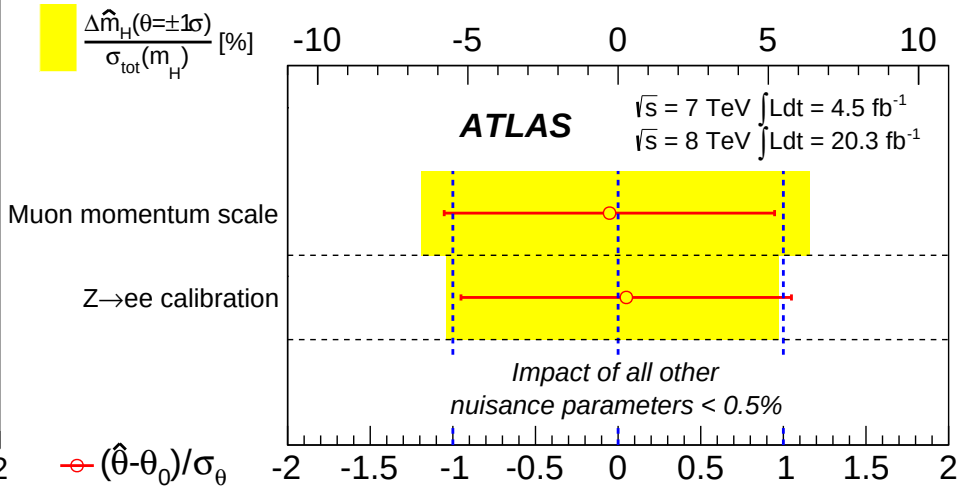

Systematics $H \to \gamma\gamma$ breakdown

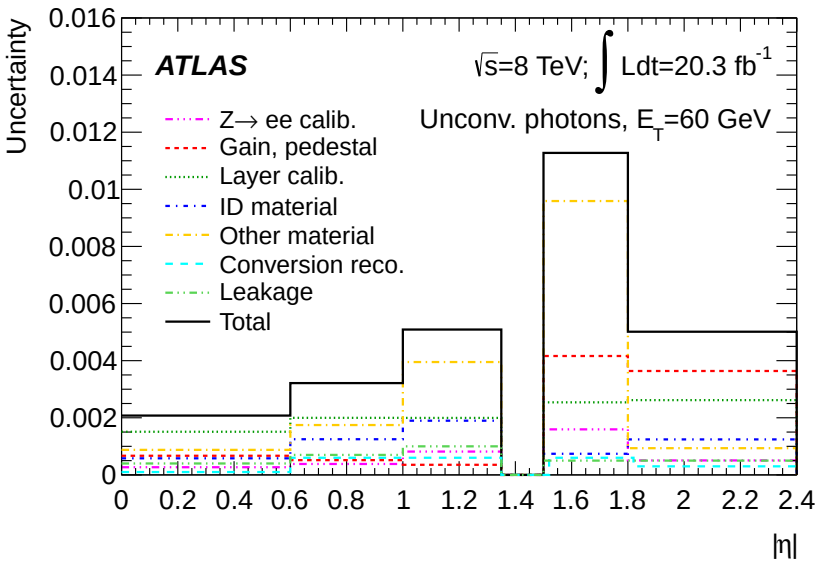

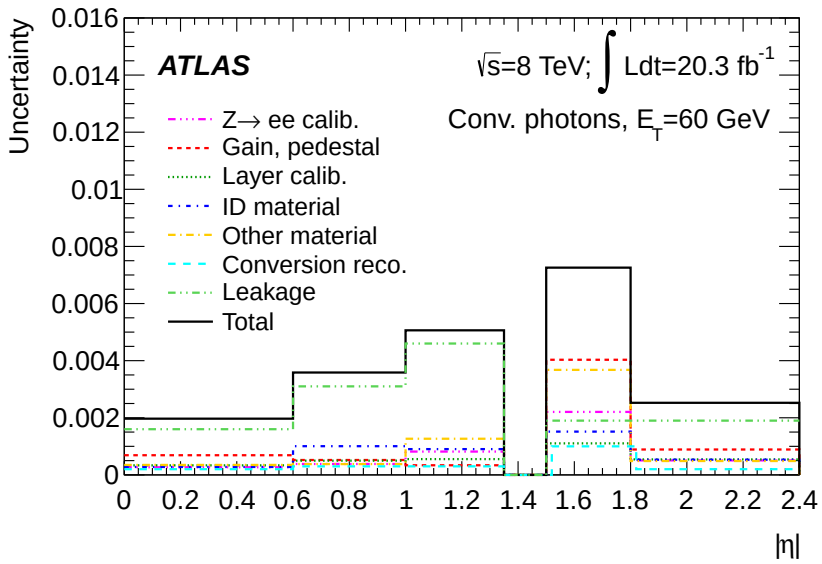

Comparison old/new $H \to \gamma\gamma$ mass

- From the changes in the calibration procedure an average shift of about -0.45 GeV is expected
- An expected statistical spread of about 0.35 GeV from fluctuations in the measured masses of individual events
- The average shift between the old and new calibrations is estimated from the distribution of the mass difference of the common events in the mass sidebands outside the signal region.

Scale factors and smearing constant term

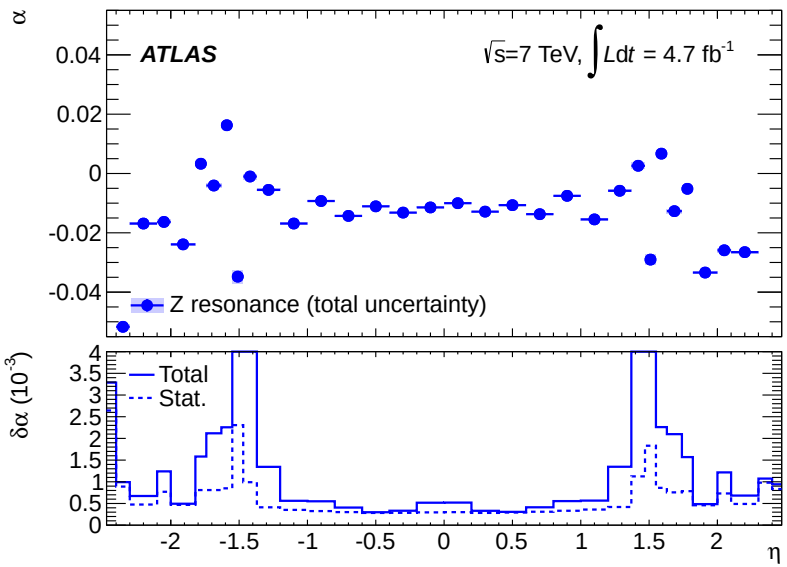

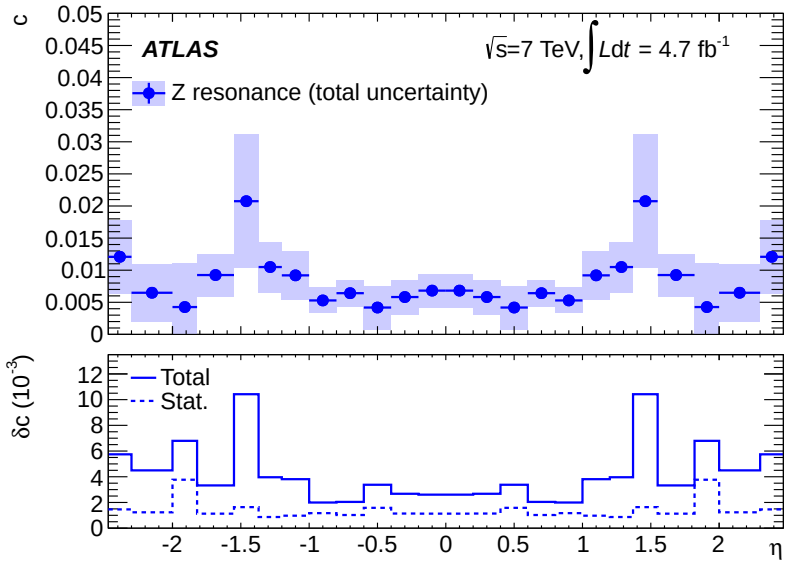

Compatibility

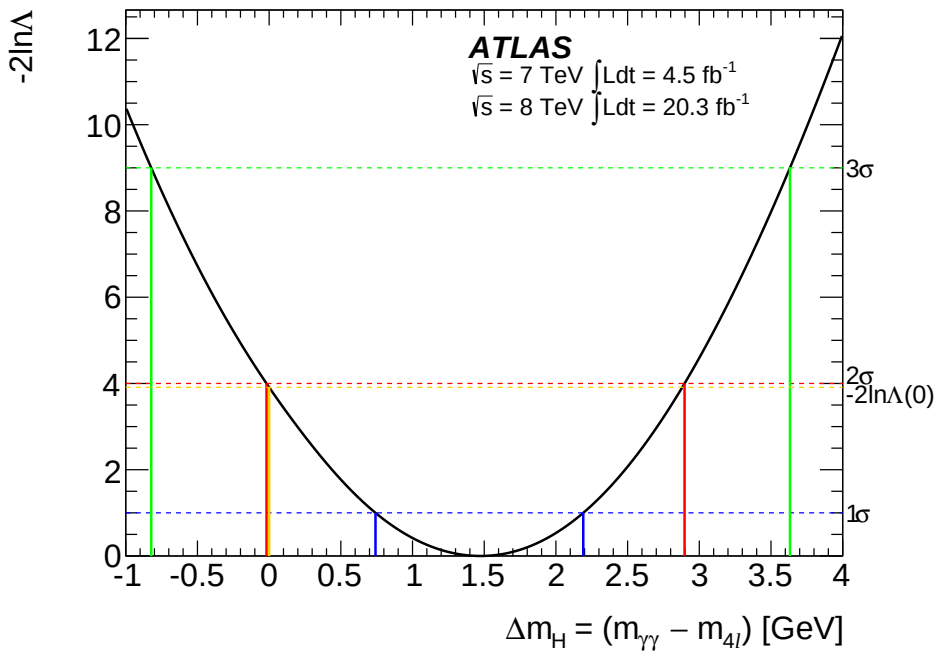

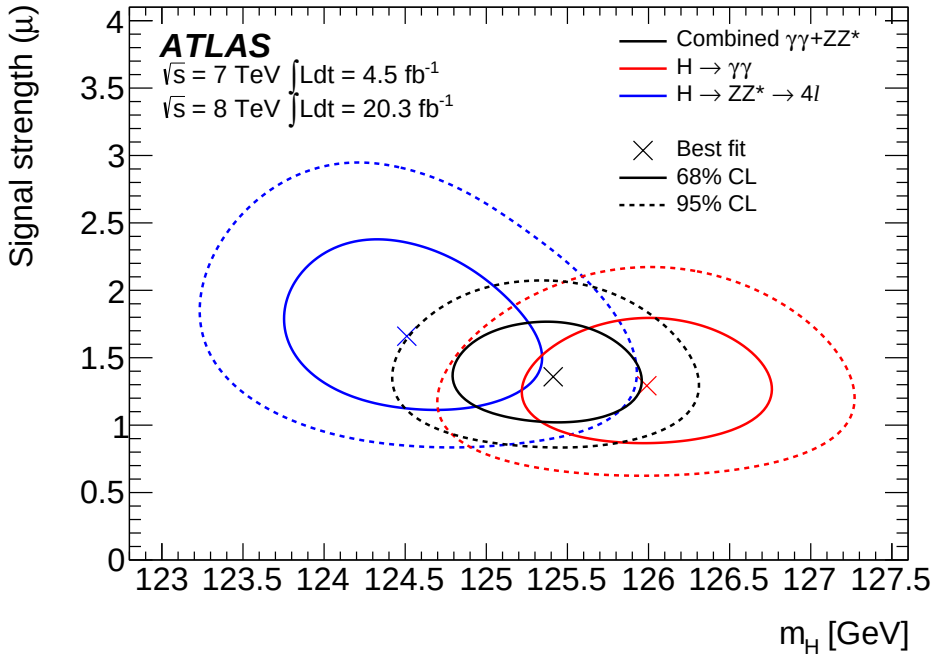

Muon momentum calibration

- p_T is measured by Inner Detector (ID) (only $|\eta| < 2.5$) and MS Spectrometer (MS) (only $0.1 < |\eta| < 2.7$).
- p_T-scale corrected comparing simulation and data $J/\psi/Z \to \mu\mu$
  - ID p_T-scale $< 0.1\%$. ID momentum systematic $0.02\%(\eta = 0) \div 0.2\%(|\eta| > 2)$
  - MS p_T-scale $-0.4\% \div +0.3\%$. MS momentum systematic $\lesssim 0.1\% \div 0.2\%$.
- combining ID and MS, systematics on p_T-scale 0.04% (barrel) $\div$ 0.2% ($\eta > 2$)
  - new inclusion of J/ψ allows for a significant reduction in the $H \to 4\ell$ p_T-region

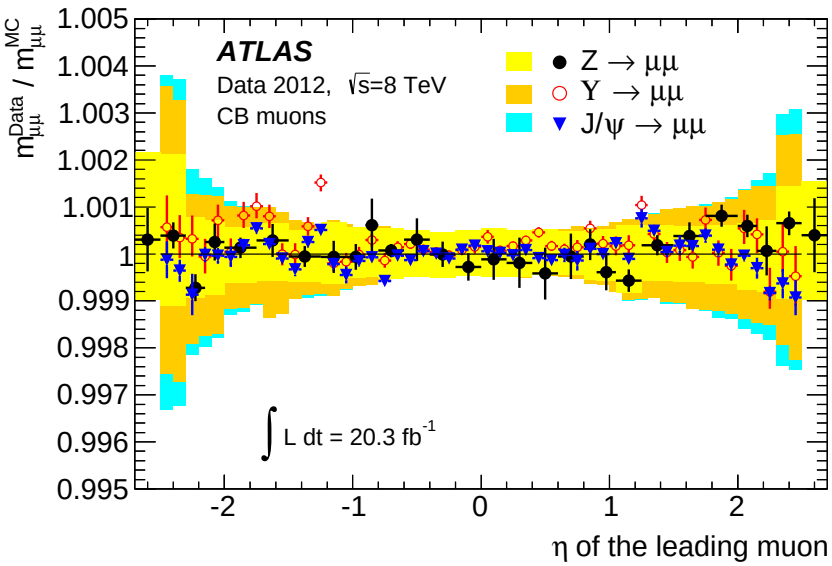

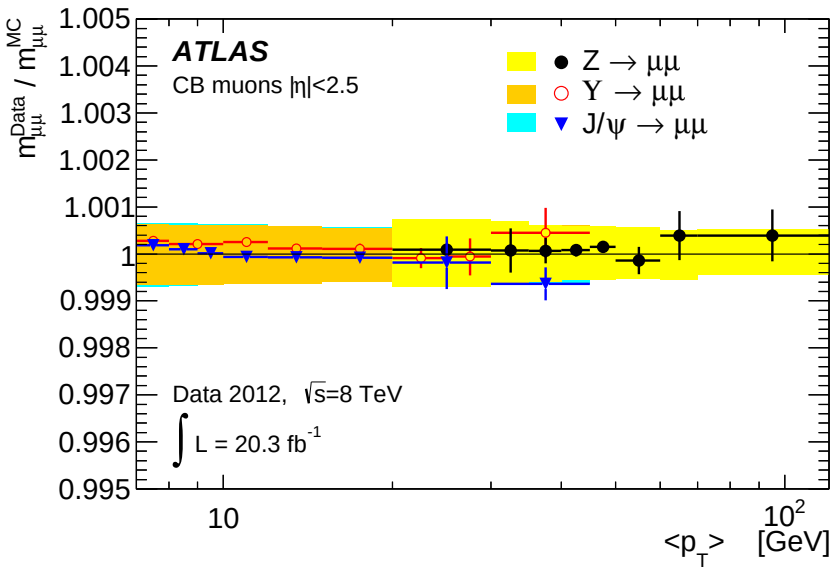

- p_T-dependent smearing correction to match resolution in data